Journal of Thermal Analysis and Calorimetry, Vol. 56 (1999) 991-1004

MODULATED DIFFERENTIAL SCANNING CALORIMETRY
Analysis of interphases in multi-component polymer materials

M. Song[1], *D. J. Hourston*[1*], *M. Reading*[1], *H. M. Pollock*[2] *and*
A. Hammiche[2]

[1]IPTME, Loughborough University, Loughborough LE11 3TU
[2]School of Physics and Chemistry, Lancaster University, UK

Abstract

A modulated-temperature differential scanning calorimetry (M-TDSC) method for the analysis of interphases in multi-component polymer materials has been developed further. As examples, interphases in a polybutadiene natural rubber (50:50 by mass) blend, a poly(methyl methacrylate)–poly(vinyl acetate) (50:50 by mass) structured latex film, a polyepichlorohydrin–poly(vinyl acetate) bilayer film, and polystyrene–polyurethane (40:60 by mass) and poly(ethyl methacrylate)–polyurethane (60:40 by mass) interpenetrating polymer networks were investigated. The mass fraction of interphase and its composition can be calculated quantitatively. These interphases do not exhibit clear separate glass transition temperatures, but occur continually between the glass transition temperatures of the constituent polymers.

Keywords: interfaces, interpenetrating polymer networks, latex, M-TDSC, polymer blends

Introduction

The interphase between two polymers, whether partially compatible or incompatible, is a region of finite thickness within which the composition varies continuously from one bulk phase to the other. This interfacial region, called the interphase, is formed by interdiffusion of the two phases, driven by the chemical potential gradient. In an incompatible system, the equilibrium interfacial thickness is attained when the entropy contribution equals the enthalpy effect [1–4], giving a thickness of typically 1–20 nm, depending on the degree of compatibility [1–5]. Polymer–polymer interphases affect mechanical properties. Applications where polymer–polymer interphases are important include rubber-toughened polymer composites and welding [6, 7]. The formation of a diffuse interphase is important in adhesion [1–5], phase separation and morphology in polymer blends [8–10], welding [11] and co-extrusion [12]. In these applications, the final properties of the polymer are substantially determined by the thickness of the interphase or the concentration profile of the two polymers across that interphase.

---

* Author to whom all correspondence should be addressed.

1418–2874/99/ $ 5.00

Akadémiai Kiadó, Budapest
Kluwer Academic Publishers, Dordrecht

Over the past twenty years or more, a substantial effort has gone into analysing the detailed morphology of interpenetrating polymer networks (IPNs). The fundamental phenomenon associated with all IPNs is the phase separation process occurring during IPN formation. However, the extent of phase separation is limited by the spatial scale over which interpenetration occurs at the onset of phase separation, and this, in turn, is related to the rates of polymerisation. IPN properties are very sensitive to preparation conditions. One can, in principle, achieve materials with different properties by varying only the synthesis conditions. IPN properties will be determined by phase continuity, domain size and the interphase.

Transmission electron microscopy (TEM) can be used to analyse domain size, domain distribution and phase continuity [13]. Small angle X-ray and neutron scattering techniques can be used to obtain information about the interphase [14–16]. However, scattering methods are not always available for the study of interface in IPNs [17, 18]. To address this problem, new techniques are needed. Two approaches reported recently by Meyer *et al.* [19] and Winnik *et al.* [20], involve solid-state NMR spin-diffusion [19] and direct non-radiative energy transfer [20] experiments to study the degree of mixing in the various phases. Meyer *et al.* [19] estimated the degree of mixing in IPNs based on the measurements of the solid state NMR spin-lattice relaxation times. The results gave information about the intimacy of mixing of the two polymer networks. Winnik *et al.* [20] also calculated the extent of component mixing in IPNs quantitatively based on the analysis of direct non-radiative energy transfer measurements. They compared the results obtained from direct non-radiative energy transfer measurements with those of dynamic mechanical analysis which were calculated by the Fox equation [20] based on the glass transition temperature values. They were in good agreement with the dynamic mechanical analysis. These analyses were based on a two-phase model. These studies are very important from an academic point of view. However, in some cases, it is difficult to describe the morphology of IPNs using just a two-phase model.

Recently, Hourston *et al.* [21] have developed a new signal, the differential of heat capacity with temperature, dC_p/dT, signal from modulated-temperature differential scanning calorimetry (M-TDSC). For the study of polymer–polymer miscibility, a basic limitation of the utility of glass transition determination exists with blends composed of components which have similar (<15°C difference) glass transition temperatures, where resolution of the T_gs by conventional DSC and dynamic mechanical thermal analysis is impossible [22, 23]. Also, for small concentrations (less than 10%) the weak transition signal is difficult to resolve [22, 23]. This limitation is reduced when M-TDSC is used. We have shown that when the difference in T_g is about 10°C [24], the dC_p/dT with temperature signal given by M-TDSC may be used to characterise polymer–polymer miscibility with high resolution. Mass fractions as low as 7% in multi-phase polymeric materials can also be determined [21]. This provides a new quantitative method for the composition analysis of multi-component polymeric materials.

In this paper, we have developed the method for the analysis of multi-component polymer materials further in an attempt to provide a valuable analysis method for determination and quantification of interphases in such materials.

Experimental

Materials and preparation

Poly(butadiene) (BR1) was obtained from Aldrich. Natural rubber (NR) was kindly provided by Enichem Elastomers Ltd. The poly(butadiene)–natural rubber (50:50 by mass) blend was prepared by using Haake Rheocord at 130°C with a rotor speed of 40 rpm. The mixing time was 12 min.

The preparation of the poly(methyl methacrylate) (PMMA)–poly(vinyl acetate) (PVAc) (50:50) structured latex film [25], the grafted polystyrene (PS)–polyurethane (PU) (40:60) IPN [26] and the poly(ethyl methacrylate)–PU (60:40) IPN [27] plus the bilayer film of polyepichlorohydrin (PECH) and poly(vinyl acetate) (PVAc) [28] were described in detail in previous paper.

Instrumentation M-TDSC

A TA Instruments M-TDSC (2910) calorimeter was used. An oscillation amplitude of 1.0°C for the structural latex film and the rubber–rubber blend, and 1.5°C for the IPNs and the PECH–PVAc bilayer films, respectively, were used. An oscillation period of 60 s and a heating rate of 3°C min^{-1} were used for all samples. The calorimeter was calibrated as a conventional DSC with a standard indium sample.

Results

Figures 1 and 2 show the change of heat capacity and dC_p/dT *vs.* temperature signals for the BR1–NR (50:50) blend prepared by melt blending and for a physical mixture of the two samples [BR1+NR (50:50)], respectively. From Fig. 1, a characteristic behaviour in the decrease of increment of heat capacity, ΔC_p, at the glass transition temperature of both polymers can be seen in the melt blend. The value of ΔC_p for a component is proportional to its mass fraction in the system under investigation. The heat capacity *vs.* temperature signal can not provide information about that interphase glass transition or its composition distribution. However, the dC_p/dT *vs.* temperature signal can provide that information.

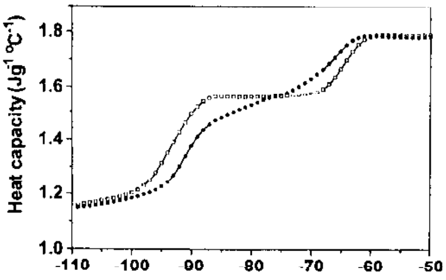

Fig. 1 Heat capacity *vs.* temperature for the BR1+NR (50:50) physical blend (–□–) and the BR1–NR (50:50) melt blend (–■–)

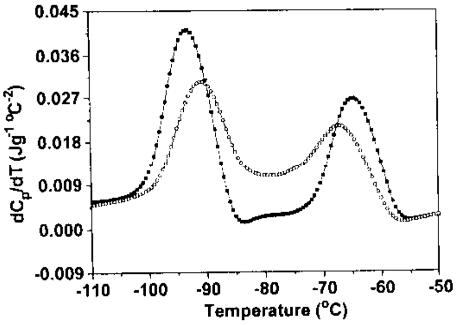

Fig. 2 dC_p/dT *vs.* temperature for the BR1+NR (50:50) physical blend (–■–) and the BR1–NR (50:50) melt blend (–○–)

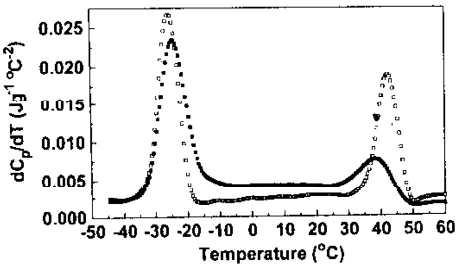

Fig. 3 dC_p/dT *vs.* temperature for the PECH–PVAc bilayer film after 0 and 1180 min annealing at 100°C; ■ – 0 min, □– 180 min

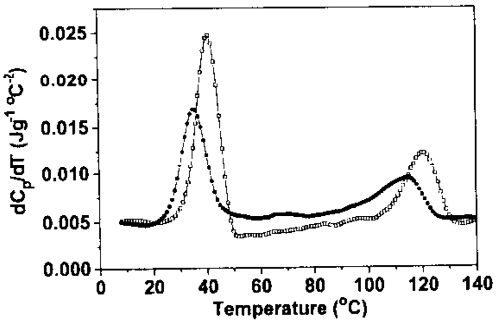

Fig. 4 dC_p/dT *vs.* temperature for the PMMA+PVAc (50:50) latex blend (–□–) and the PMMA–PVAc (50:50) structured latex film (–●–)

Figures 3–6 show the dC_p/dT *vs.* temperature signals for a diffuse interphase in the PECH–PVAc bilayer film after annealing for 1180 min at 100°C, for the PMMA–PVAc (50:50) structured latex film and the physical mixture (50:50) of the

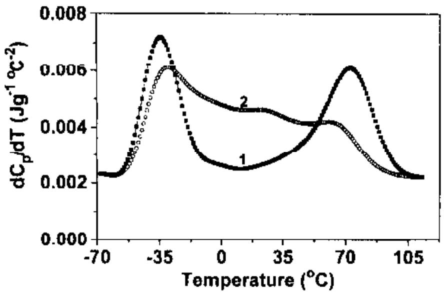

Fig. 5 dC_p/dT *vs.* temperature for the PEMA (60%)+PU (40%) physical blend (1) and the PEMA (60%)–PU (40%) IPN (2)

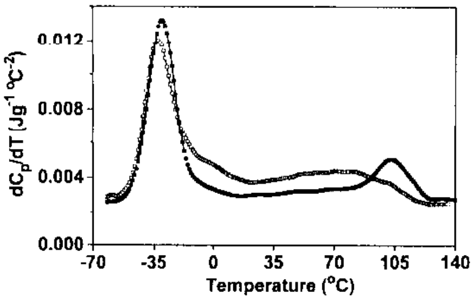

Fig. 6 dC_p/dT *vs.* temperature for the PU (60%)+PS (40%) physical blend (-■-) and the PU (60%)–PS (40%) IPN (-□-)

equivalent constituent latexes (PMMA and PVAc), for the PEMA (60%)–PU (40%) IPN and the physical mixture of its constituent networks [PEMA (60%)+PU (40%)] and for the PU (60%)–PS (40%) IPN and the physical mixture of its constituent networks [PU (60%)+PS (40%)]. These results show that the values of the dC_p/dT *vs.* temperature signal for the thermally treated PECH–PVAc bilayer film, the structured latex film and the IPN samples are larger than that for polymer 1+polymer 2 samples (physical blends) between the glass transition temperatures of polymer 1 and polymer 2. The heat-treated PECH–PVAc bilayer film has a single interphase. It is clear that this interphase does not exhibit a separate glass transition temperature, but occurs continually between the glass transition temperatures of the constituent polymers.

Analysis

Description of dC_p/dT vs. temperature signal for multi-phase polymer materials

A differential equation to describe the kinetics of enthalpy (H) relaxation for conventional differential scanning calorimetry (DSC) has been suggested by Kovacs *et al.* [29]. It is shown below as Eq. (1):

$$\frac{\mathrm{d}\delta}{\mathrm{d}t}=\Delta C_p q-\frac{\delta}{\tau(T,\delta)} \tag{1}$$

where δ ($=H-H_\infty$) is the excess enthalpy relative to the equilibrium value (H_∞), ΔC_p is the difference between the liquid (C_p^l) and glassy (C_p^g) specific heat capacities, q is the heating rate and t is time.

The single relaxation time, τ, depends [29] upon both T and δ, according to Eq. (2):

$$\tau=\tau_g\exp[-\theta(T-T_g)]\exp\left[-(1-x)\frac{\theta\delta}{\Delta C_p}\right] \tag{2}$$

where τ_g is the equilibrium relaxation time at the glass transition temperature, T_g, x is the non-linearity parameter ($0\leq x\leq 1$), and θ is a constant defining the temperature dependence of τ, which is given by the approximation

$$\theta=\frac{\Delta h^*}{RT_g^2} \tag{3}$$

where Δh^* is an apparent activation energy. Equations (1) and (2) define the response of the glass to any prescribed thermal history. The following approximate equation [29] will be used in this paper for the relaxation time τ:

$$\tau=\tau_g\exp[-\theta(T-T_g)] \tag{4}$$

For M-TDSC [30],

$$\frac{\mathrm{d}Q}{\mathrm{d}t}=C_{pt}\frac{\mathrm{d}T}{\mathrm{d}t}+f(t,T)-qC_{pt}+<f(t,T)>+\omega A_T C_{pt}\cos(\omega t)+C\sin(\omega t) \tag{5}$$

where $\mathrm{d}Q/\mathrm{d}t$ is the heat flow into the sample, A_T is the amplitude of the temperature modulation, ω is the frequency of modulation, C_{pt} is the reversing heat capacity of the sample due to its molecular motions at the heating rate q, $f(t,T)$ is the heat flow arising as a consequence of any kinetically-retarded event, $<f(t,T)>$ is the average of $f(t,T)$ over the interval of as least one modulation and C is the amplitude of the kinetically retarded response to the temperature modulation.

Consider the complex heat capacity, C_p^*, which can be divided into two parts: a real part, C_p, and an imaginary part, C_p''.

$$C_p^*=C_p-\mathrm{i}C_p'' \tag{6}$$

Assuming $C_p=A+BT+f(T)$ during the glass transition [26], according to Reading *et al.* [30], C_p has been obtained as follows.

$$C_p=A+BT+\frac{\Delta C_p}{1+\omega^2\tau_g^2\exp\left[\frac{-2\Delta h^*}{RT_g^2}(T-T_g)\right]} \tag{7}$$

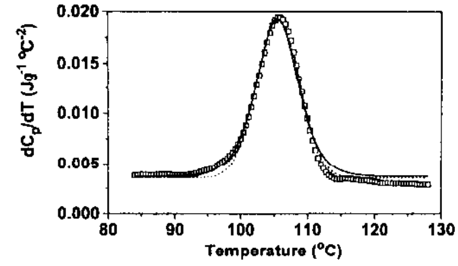

Fig. 7 Comparison of dC_p/dT *vs.* temperature experimental data (square points) with theoretical (solid line) and a Gaussian function (dots) for polystyrene

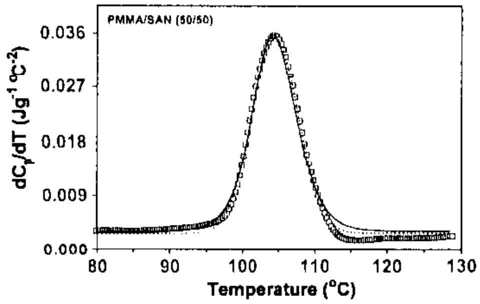

Fig. 8 Comparison of dC_p/dT *vs.* temperature experimental data (square points) with theoretical (solid line) and a Gaussian function (dots) for a miscible blend of poly(methyl methacrylate) and poly(styrene-co-acrylonitrile) (50:50) by mass)

Figures 7 and 8 give a comparison of the dC_p/dT *vs.* temperature data for experimental (square points), theoretical (solid line) and a Gaussian function (dots) for PS and a 50/50, by mass miscible blend of poly(methyl methacrylate) and poly(styrene-co-acrylonitrile) [24]. Obviously, the experimental data at the glass transition can be described by the theory, and also well by a Gaussian function. In this paper, we use a Gaussian function to describe the change of dC_p/dT *vs.* temperature at the glass transition for the analysis of the morphology of multi-component polymer materials.

Baseline correction of the dC_p/dT signals from multi-phase-systems

From the above analysis, it is clear that the dC_p/dT *vs.* temperature signal can be described by a Gaussian function for polymers and miscible polymer blends. However, the dC_p/dT *vs.* temperature signals for the polymer 1+polymer 2 physical blends can not be described well by the sum of two Gaussian functions because of the shift of the baseline between the glass transition temperatures. Therefore, the dC_p/dT *vs.* temperature signal includes a non-constant baseline for multi-phase systems. Because a Gaussian function was used for the quantitative analysis of interphase in these multi-phase systems, the non-constant baseline had to be corrected.

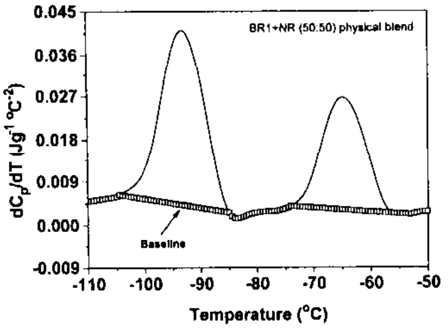

Fig. 9 Illustration of the baseline selection for the dC_p/dT *vs.* temperature signal analysis

The values of the dC_p/dT *vs.* temperature signal for polymer 1+polymer 2 physical blends above and below the two glass temperatures are considered as the baseline for the dC_p/dT signal of these multi-phase systems. For the glass transitions, baselines which are linear with temperature from the starting and end points of the glass transition temperature were chosen. An example is given shown in Fig. 9. Thus, for the BR1–NR (50:50) blend, a baseline, labelled in Fig. 9 was used. When the dC_p/dT *vs.* temperature signal is analysed using a multi-Gaussian function for multi-phase systems, this baseline must be subtracted from the raw dC_p/dT *vs.* temperature signal.

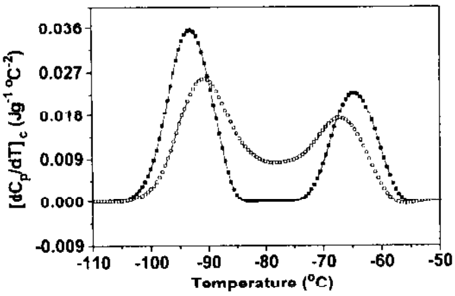

Fig. 10 Corrected dC_p/dT *vs.* temperature for the BR1+NR (50:50) physical blend (-■-) and the BR1–NR (50:50) melt blend (–o–)

Figures 10–14 show the corrected differential of heat capacity, $[dC_p/dT]_c$ *vs.* temperature signal for the BR1–NR (50:50) blend and the BR1+NR (50:50) physical blend, for the diffuse interphase of the PECH–PVAc bilayer films after 0 and 1180 min at 100°C, for the PMMA–PVAc (50:50) structured latex film and the PMMA+PVAc (50:50) latex blend, for the PEMA (60%)–PU (40%) IPN and the PEMA (60%+PU (40%) network physical blend, and for the PU (60%)–PS (40%) IPN and the PU (60%)+PS (40%) network physical blend, respectively.

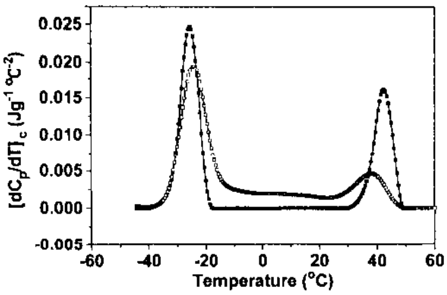

Fig. 11 Corrected dC_p/dT *vs.* temperature for the PECH–PVAc bilayer film after 0 min (-■-) and 1180 min (-□-) annealing at 100°C

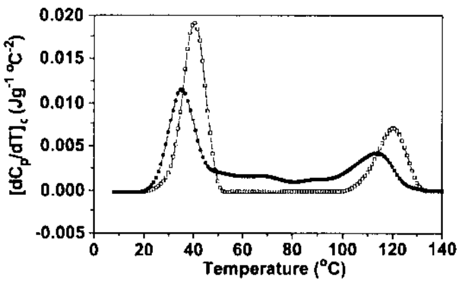

Fig. 12 Corrected dC_p/dT *vs.* temperature for the PMMA+PVAc (50:50) latex blend (—□—) and the PMMA-PVAc (50:50) structured latex film (—●—)

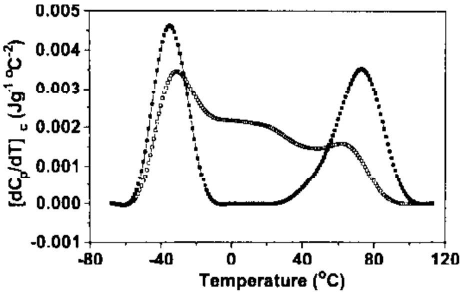

Fig. 13 Corrected dC_p/dT *vs.* temperature for the PEMA (60%)+PU (40%) physical blend (-□-) and PEMA (60%)-PU (40%) IPN (-■-)

Analysis

For polymers and miscible polymer blends, the dC_p/dT *vs.* temperature signal can be described by a Gaussian function, G, of temperature, the increment of heat capac-

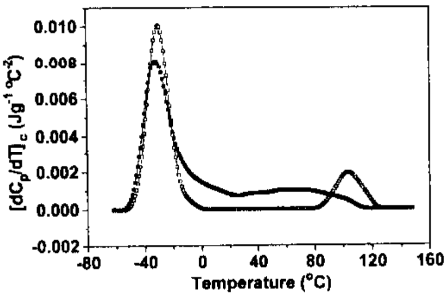

Fig. 14 Corrected dC_p/dT *vs.* temperature for the PU (60%)+PS (40%) physical blend (–□–) and the PU (60%)–PS (40%) IPN (–■–)

ity, ΔC_p, the glass transition temperature, T_g, and the half width, ω_d, of the glass transition [26].

$$G=\frac{\Delta C_p}{\omega_d\left(\frac{\pi}{2}\right)^{1/2}}\exp\left[\frac{-2(T-T_g)^2}{\omega_d^2}\right] \tag{8}$$

For a multi-phase system it has been considered that G is a multiple Gaussian function in the transition region [26].

$$\begin{aligned}G &= \sum_i G_i(T,T_{gi},\omega_{di},\Delta C_{pi})\\ &= \Delta C_{p1}/[\omega_{d1}(\pi/2)^{1/2}]\exp[-2(T-T_{g1})^2/\omega_{d1}^2]\\ &+ \Delta C_{p2}/[\omega_{d2}(\pi/2)^{1/2}]\exp[-2(T-T_{g2})^2/\omega_{d2}^2]\\ &+ \Delta C_{p3}/[\omega_{d3}(\pi/2)^{1/2}]\exp[-2(T-T_{g3})^2/\omega_{d3}^2] + \ldots\end{aligned} \tag{9}$$

where $G_i(T)$ is related to its phase of the multi-phase system. The total ΔC_p is the sum of ΔC_{pi} of each phase.

$$\Delta C_p = \sum_i \Delta C_{pi} \tag{10}$$

The glass transition temperature as a function of distance from a discrete phase boundary between polystyrene and poly(bisphenol-A carbonate) has been studied theoretically [31]. Consider that the interfacial phase is divided into N sub-systems. Each sub-system has an average composition $\{<\varphi^1>, <\varphi^2>, \ldots <\varphi^n>\}$, as shown in Fig. 15. For these N sub-systems, there is a glass transition temperature spectrum, $\{T_g^1, T_g^2, T_g^3 \ldots T_g^n\}$. Assume that the dC_p/dT signal for the glass transition process of each sub-system can be described by Eq. (8). For the glass transition temperature spectrum, the dC_p/dT signal is as follows:

$$\left(\frac{\mathrm{d}C_\mathrm{p}}{\mathrm{d}T}\right)_{\mathrm{interphase}}=\sum\frac{\mathrm{d}C_{\mathrm{pi}}^{\mathrm{g}}}{\mathrm{d}T}=\sum\frac{\Delta C_{\mathrm{pi}}^{\mathrm{g}}}{\omega_{\mathrm{di}}^{\mathrm{g}}(\pi/2)^{1/2}}\exp\left[\frac{-2(T-T_{\mathrm{gi}}^{\mathrm{g}})^2}{(\omega_{\mathrm{di}}^{\mathrm{g}})^2}\right] \qquad (11)$$

where $\Delta C_{\mathrm{pi}}^{\mathrm{g}}$ is the increment of heat capacity, $T_{\mathrm{gi}}^{\mathrm{g}}$ is the glass transition temperature and $\omega_{\mathrm{di}}^{\mathrm{g}}$ is the half width of the glass transition for *i*th sub-system.

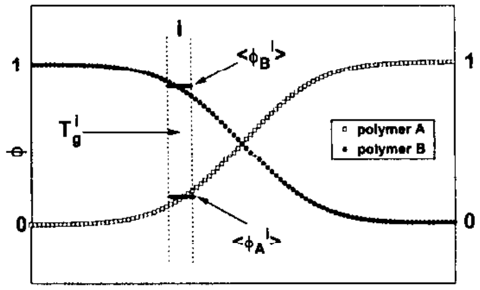

Fig. 15 Schematic of composition profile in an interphase

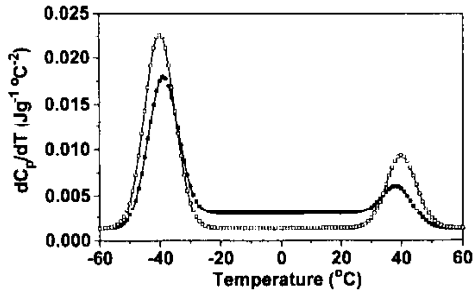

Fig. 16 Prediction of the $\mathrm{d}C_\mathrm{p}/\mathrm{d}T$ *vs.* temperature signals for two-phase systems; with a diffuse interphase (–■–) and without a diffuse interphase (–□–)

Figure 16 shows the $\mathrm{d}C_\mathrm{p}/\mathrm{d}T$ *vs.* temperature signal for a diffuse interphase in a two-component polymer system calculated by Eq. (11). Here it is assumed that the difference between T_{g1} and T_{g2} is 80°C. The diffuse interphase was divided into 7 sub-systems. Assume that the mass fraction of the interphase is 20%, and ΔC_{p1} and ΔC_{p2} are 0.4 and 0.2 J g^{-1} $°\mathrm{C}^{-1}$ for polymer 1 and polymer 2, respectively. The parameters used for this model are shown in Table 1. The peak position of the $\mathrm{d}C_\mathrm{p}/\mathrm{d}T$ *vs.* temperature signal for the polymer 1-rich phase is slightly shifted to higher temperature and that for the polymer 2-rich phase shifted slightly to lower temperature. This results from peak overlapping.

For such a diffuse phase system, the corrected *G* function can be rewritten as follows:

$$G=\left(\frac{\mathrm{d}C_\mathrm{p}}{\mathrm{d}T}\right)_{\text{polymer 1-rich phase}}+\left(\frac{\mathrm{d}C_\mathrm{p}}{\mathrm{d}T}\right)_{\text{polymer 2-rich phase}}+\sum\frac{\Delta C_{\mathrm{pi}}^{\mathrm{g}}}{\omega_{\mathrm{di}}^{\mathrm{g}}(\pi/2)^{1/2}}\exp\left[\frac{-2(T-T_{\mathrm{gi}}^{\mathrm{g}})^2}{(\omega_{\mathrm{di}}^{\mathrm{g}})^2}\right] \quad (12)$$

Using Eq. (12) and the peak resolution technique, the interphase can be analysed quantitatively. Figure 17 shows the results of peak resolution for the PMMA–PVAc structured latex film.

Table 1 Modeling parameters (see Fig. 16)

Sub-system	T_g^g/°C	Mass fraction	$\Delta C_\mathrm{p}^\mathrm{g}$/J g^{-1} °C^{-1}
1	–30	0.0286	0.0107
2	–20	0.0286	0.0100
3	–10	0.0286	0.0093
4	0	0.0286	0.0086
5	10	0.0286	0.0078
6	20	0.0286	0.0071
7	30	0.0286	0.0064

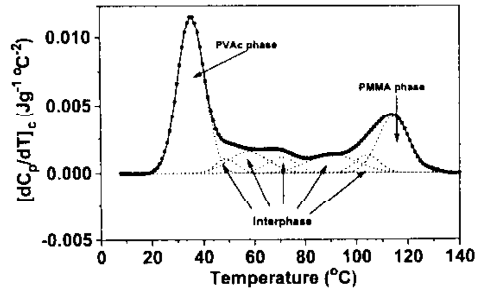

Fig. 17 Peak resolution results for the PMMA–PVAc (50:50) structured latex film

Table 2 Mass fractions (%) of the polymer 1-rich, polymer 2-rich phases and interphases in the BR1 (polymer 1)–NR (polymer 2) blend, the PECH (polymer 1)–PVAc (polymer 2) bi-layer film, the PMMA (polymer 1)–PVAc (polymer 2) (50:50) structured latex film and the PEMA (60%) (polymer 1)–PU (40%) (polymer 2) and the PU (60%) (polymer 1)–PS (40%) (polymer 2) IPN systems

Sub-system	Polymer 1/%	Polymer 2/%	Interphases/%
BR1–NR	40	39	21
PECH–PVAc	42	36	22
PMMA–PVAc	31	26	43
PEMA–PU	19	22	59
PU–PS	32	19	49

Table 2 shows the mass fractions of polymer 1-rich phase, polymer 2-rich phase and the interphases in the BR1–NR, the PECH–PVAc bilayer film, the PMMA–PVAc (50:50) latex film, the PEMA (60%)–PU (40%) IPN and the PU (60%)–PS (40%) IPN systems.

Conclusions

The M-TDSC dC_p/dT *vs.* temperature signal is a useful tool for characterising the morphology of multi-phase polymers. Calibrated dC_p/dT *vs.* temperature signals can be used quantitatively to analyse interphases, in terms of mass fraction and component composition in multi-component polymer materials. These interphases do not exhibit separate glass transition temperatures, but occur continuously between the glass transition temperatures of the two constituent polymers.

* * *

Drs H. Z. Zhang and F.-U. Schafer of Loughborough University are thanked for providing the IPN and latex samples, respectively.

References

1 S. Wu, Polymer Interface and Adhesion, Dekker, N. Y. 1982.
2 P. Helfand and Y. Tagami, J. Chem. Phys., 56 (1972) 3592.
3 K. M. Hong and J. Noolandi, Macromolecules, 15 (1982) 482.
4 C. I. Poser and I. C. Sanchez, Macromolecules, 24 (1984) 79.
5 N. H. Sung, A. Kaul, I. Chin and C. S. P. Sung, Polym. Eng. Sci., 22 (1982) 637.
6 K. Binder and H. Sillescu, in Encyclopedia of Polymer Science and Engineering, Wiley, N. Y. 20 (1989) 297.
7 H. H. Kausch and M. Tirrell, Ann. Rev. Mater. Sci., 19 (1989) 341.
8 T. K. Kwei and T. T. Wang, in Polymer Blends, Vol. 1, D. R. Paul and S. Newman Eds., Academic Press, N. Y. 1978.
9 H. van Oene, in Polymer Blends, Vol. 1, D. R. Paul and S. Newman Eds., Academic Press, N. Y. 1978.
10 S. Wu, presented at 16th Europhysics Conference on Macromolecules, Polymer Alloys: Structure and Properties, Brugge, 1984.
11 Y. H. Kim and R. P. Wool, Macromolecules, 16 (1983) 1115.
12 C. D. Han, Multiphase Flow in Polymer Processing, Academic Press, N. Y. 1981.
13 L. H. Sperling, Interpenetrating Polymer Networks and Related Materials, Plenum Press, N. Y. 1981.
14 S. B. Pandit and V. M. Nadkarni, Macromolecules, 27 (1994) 4583.
15 T. P. Russell, D. S. Lee, T. Nishi and S. C. Kim, Macromolecules, 26 (1993) 1922.
16 V. V. Shilov, Y. S. Lipatov, L. V. Karabanova and L. M. Sergeeva, J. Polym. Sci., Polym. Chem. Ed., 17 (1979) 3083.
17 M. Song, D. J. Hourston and F.-U. Schafer, Submitted for publication in Polymer, 1998.
18 S. Tan, D. Zhang and E. Zhou, Polymer, 38 (1997) 4571.
19 N. Parizel, G. Meyer and G. Weill, Polymer, 36 (1995) 2323.
20 J. Yang, M. K. Winnik, D. Ylitalo and R. J. De Voe, Macromolecules, 29 (1996) 7055.
21 D. J. Hourston, M. Song, A. Hammiche, H. M. Pollock and M. Reading, Polymer, 38 (1997) 1.
22 O. Olabisi, L. Robeson and M. T. Shaw, Polymer–Polymer Miscibility, Academic Press, N. Y. 1979.

23 M. J. Folkes and P. S. Hope, Polymer Blends and Alloys, Blackie Academic and Professional, London 1993.

24 M. Song, A. Hammiche, H. M. Pollock, D. J. Hourston and M. Reading, Polymer, 36 (1995) 3315.

25 D. J. Hourston, H. X. Zhang, M. Song, M. H. Pollock and A. Hammiche, Thermochim. Acta, 294 (1997) 23.

26 M. Song, D. J. Hourston, F. U. Schafer, H. M. Pollock and A. Hammiche, Thermochim. Acta, 315 (1998) 25.

27 D. J. Hourston and F. U. Schafer, J. Appl. Polym. Sci., 62 (1997) 2025.

28 M. Song, H. M. Pollock, A. Hammiche, D. J. Hourston and M. Reading, Polymer, 38 (1997) 503.

29 A. J. Kovacs and J. M. Hutchinson, J. Polym. Sci., Polym. Phys., 14 (1976) 1575.

30 K. J. Jones, I. Kinshott, M. Reading, A. A. Lacey, C. Nikolopoulos and H. M. Pollock, Thermochim. Acta, 304/305 (1997) 187.

31 D. Porter, Group Interaction Modelling of Polymer Properties, Dekker, New York 1995.